Journal of
Water & Climate Change

IWA PUBLISHING

Journal of Water and Climate Change Vol 12 No 7, 3159 doi: 10.2166/wcc.2021.137

Impact of climate change on hydro-meteorological drought over the Be River Basin, Vietnam

Dao Nguyen Khoi[a,b], Truong Thao Sam[a,c], Pham Thi Loi[a,b], Bui Viet Hung[a,b] and Van Thinh Nguyen[d,*]

[a] Faculty of Environment, University of Science, Ho Chi Minh City 700000, Vietnam
[b] Vietnam National University, Ho Chi Minh City 700000, Vietnam
[c] Institute for Computational Science and Technology, Ho Chi Minh City 700000, Vietnam
[d] Department of Civil and Environmental Engineering, Seoul National University, 1 Gwanak-ro, Gwanak-gu, Seoul 151-744, Korea
*Corresponding author. E-mail: vnguyen@snu.ac.kr

ABSTRACT

In this paper, the responses of hydro-meteorological drought to changing climate in the Be River Basin located in Southern Vietnam are investigated. Climate change scenarios for the study area were statistically downscaled using the Long Ashton Research Station Weather Generator tool, which incorporates climate projections from Coupled Model Intercomparison Project 5 (CMIP5) based on an ensemble of five general circulation models (Can-ESM2, CNRM-CM5, HadGEM2-AO, IPSL-CM5A-LR, and MPI-ESM-MR) under two Representative Concentration Pathway (RCP) scenarios (RCP4.5 and RCP8.5). The Soil and Water Assessment Tool model was employed to simulate streamflow for the baseline time period and three consecutive future 20-year periods of 2030s (2021–2040), 2050s (2041–2060), and 2070s (2061–2080). Based on the simulation results, the Standardized Precipitation Index and Standardized Discharge Index were estimated to evaluate the features of hydro-meteorological droughts. The hydrological drought has a 1-month lag time from the meteorological drought and the hydro-meteorological droughts have negative correlations with the El Niño Southern Oscillation and Pacific Decadal Oscillation. Under the climate change impacts, the trends of drought severity will decrease in the future; while the trends of drought frequency will increase in the near future period (2030s), but decrease in the following future periods (2050 and 2070s). The findings of this study can provide useful information for the policy- and decisionmakers for a better future planning and management of water resources in the study region.

Key words: Be River Basin, climate change, hydro-meteorological drought, SWAT model

HIGHLIGHTS

- There is a lack of knowledge about how climate change will affect the hydro-meteorological drought in the tropical region.
- The hydro-meteorological droughts have negative correlations with the global climate oscillation.
- The drought frequency will have a rising trend in the near future period (2030s) and downward trends in the following future periods (2050 and 2070s).

1. INTRODUCTION

As stated in the global risks report of the World Economic Forum (WEF), extreme weather events (e.g. droughts and floods) and climate action failure have been identified as the two top high-risks, which have severely impacted on livelihoods, environment, and society (World Economic Forum 2021). Drought is defined as a prolonged period of abnormally dry weather that causes serious hydrological imbalance (IPCC 2013). The droughts focused on in this study are referred to the meteorological and hydrological droughts. The meteorological drought pertains to a deficiency in precipitation, while the hydrological drought is related to deficiencies in streamflow, groundwater, and water storage in lakes and reservoirs (Wu *et al.* 2017). The physical connection between hydrological processes results in the difference of occurrence time of hydrological and meteorological droughts (Salimi *et al.* 2021), wherein the hydrological drought normally happens after meteorological drought. Four basic parameters are used to characterize a drought, as follows: (i) duration refers to the number of drought months of an event; (ii) frequency is the number of drought months over a specified time period; (iii) intensity refers to the degree of a drought event; and (iv) severity is the ratio of the intensity to the duration (Sam *et al.* 2019).

Recently, drought frequency and severity have shown crucially rising trends caused by changing climate in both global and regional scales.

Examining the global trend of drought, Prudhomme *et al.* (2014) found that the global severity of hydrological drought has an upward trend in the future. Regarding the regional trend of drought, they also indicated that the drought frequency and severity are expected to have increased trends in South America, Western and Central Europe, Africa, and Southern Australia. In addition, Jung & Chang (2012) have revealed that the climate changing impacts on drought characteristics (severity, duration, and frequency) vary over spatial and temporal scales. Therefore, it is important to understand and assess the drought characteristics of a region in the conditions of climate change for developing mitigation and adaptation plans for natural disasters.

In recent years, many studies have been conducted to assess the impact of climate change on hydro-meteorological drought at the regional scale using hydrologic modeling tools. For instance, Blanco-Gómez *et al.* (2019) have assessed the impact of changing climate on drought in the Guajoyo River Basin (El Salvador) under five general circulation models (GCMs) using the SWAT (Soil and Water Assessment Tool), and they found that the drought duration and intensity have upward trends in the future. Zhao *et al.* (2019) used the SWAT model together with Stream Drought Index (SDI) to prognosticate the effect of changing climate on hydrological drought in the Weihe River Basin (China) and inferred the rises in frequency, duration, and intensity of hydrological drought in the future. In addition, Tan *et al.* (2019) assessed the climate change impact on meteorological and hydrological droughts in the Johor River Basin (Malaysia) using the SWAT model and two drought indices, the Standardized Precipitation Index (SPI) and the Standardized Streamflow Index (SSI), and demonstrated that the future drought will become more frequent. In general, the popular approach to examine and project the hydro-meteorological drought under the climate change impact is a modeling approach including a combination of GCM simulations, downscaling techniques, hydrological models, and drought indices.

Vietnam located in tropical Southeast Asia is considered as one of the world's most vulnerable countries to the effects of climate change and natural disasters (IPCC 2018). On the report of the World Bank (WB), approximately 60% of Vietnam's terrestrial area and 70% of its population are susceptible to natural disasters (World Bank & GFDRR 2017). The extreme weather events in Vietnam caused an approximately 0.47% loss of the annual Gross Domestic Product (GDP) over the past 20-year period (2000–2019) (Eckstein *et al.* 2021). In the 2015/2016 drought alone, Vietnam had suffered an economic loss of approximately USD$ 674 million, accounting for about 0.35% of GDP in 2015 (UNDP 2016). Recently, drought studies in Vietnam under climate change impacts have received considerable attention; however, they are mainly focused on meteorological drought (Vu-Thanh *et al.* 2014; Vu *et al.* 2015; Stojanovic *et al.* 2020), and there is still limited knowledge of climate change impacts on the hydrological drought in Vietnam. Furthermore, the interaction between the global climate oscillation (i.e. El Niño Southern Oscillation (ENSO) and Pacific Decadal Oscillation (PDO)) and the hydro-meteorological droughts is also not well known.

The main purpose of this study is to explore responses of hydro-meteorological drought to changing climate in the Be River Basin (BRB) in Vietnam. The BRB was selected for the present study because this area is identified as one of drought-affected hotspots in Vietnam (World Bank & GFDRR 2017). The outcomes of this study can provide the scientific information and knowledge of the changing climate impacts on the drought to the water managers and policymakers.

2. STUDY REGION

The present study is focused on the BRB located between latitudes 11°05′–12°25′N and longitudes 106°35′–107°30′E (Figure 1). The area of the basin is nearly 7,560 km^2, and the river has a length of approximately 331 km with an average annual discharge of about 7.9–9.0 million cubic meters. The mean discharge is about 250–300 m^3/s varied between the lowest discharge of about 60 m^3/s in the dry season and the highest discharge of about 1,000 m^3/s in the rainy season. The surface elevation of the basin ranges from 1,000 to 10 m above the mean sea level sloping along the direction from the northeast to the south. This basin has a monsoon tropical climate characterized by two distinct seasons, i.e. the dry season from November to April, and the wet season from May to October. The average annual rainfall is approximately 2,460 mm in the period 1980–2017 with the highest and lowest values recorded as 3,050 mm in 2000 and 1,585 mm in 2010, respectively. Nearly 75% of the basin area is covered by basaltic soil (Khoi *et al.* 2017), which is suited to agricultural development. The main land-use types are forest and agricultural lands. Specifically, the forest land and agricultural land in

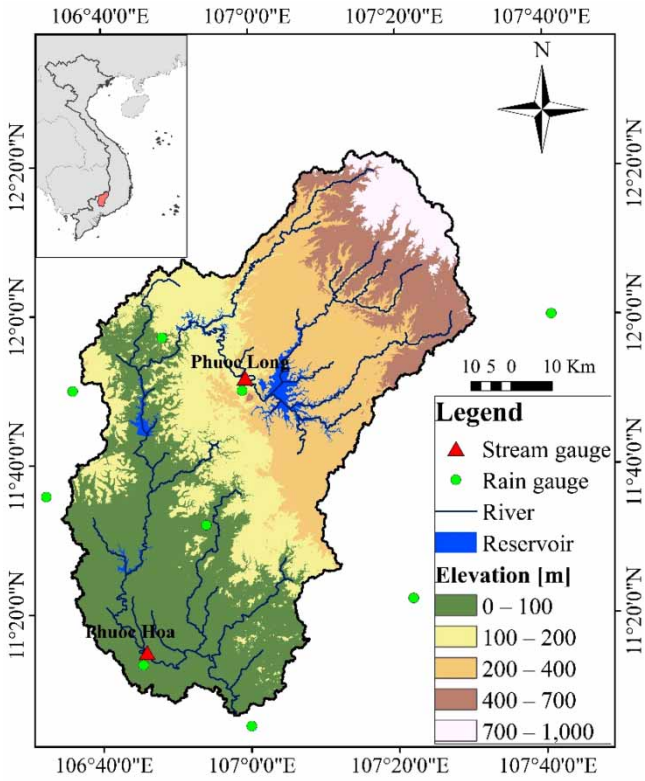

Figure 1 | Location of the BRB.

2005 covered approximately 1,591 km^2 (accounting for 20.3% of the basin area) and 5,392 km^2 (68.8% of the basin area), respectively.

3. MATERIALS AND METHODS

The SWAT model was applied to investigate the streamflow for the baseline time period (1986–2005) and three future time periods of the 2030s (2021–2040), 2050s (2041–2060), and 2070s (2061–2080). The climate change scenarios for the study area were statistically downscaled using the LARS-WG tool based on an ensemble of five GCMs (Can-ESM2, CNRM-CM5, HadGEM2-AO, IPSL-CM5A-LR, and MPI-ESM-MR) under two RCP scenarios, RCP 4.5 and RCP8.5.

3.1. SWAT model setup

The SWAT is a physically semi-distributed model used to simulate hydrological processes in the river basin scale (Neitsch *et al.* 2011). It has been promising in its application for the simulation of hydrology and hydro-meteorological extremes to a wide array of river basins of varying scales around the world, especially in Southeast Asia (Tan *et al.* 2020). In the SWAT model, a basin is divided into a number of sub-basins, which are further partitioned into hydrological response units (HRUs) based on soil, land use, and slope features. The model simulates hydrological processes using a balance equation of soil water content. The balance equation consists of hydrological components, namely precipitation, evapotranspiration, runoff, water percolation, and return flow. Full details on the SWAT model can be found in Neitsch *et al.* (2011).

There are numerous data required for the input of the SWAT model, such as topography, land-cover, soil, and hydro-meteorological data. Specifically, Shuttle Radar Topography Mission (SRTM) 30 × 30 m resolution data (https://srtm.csi.cgiar.org/srtmdata/) were implemented for delineation of basin and sub-basins. Land-cover data in 2005 with a spatial resolution of 300 m were produced by the European Space Agency (ESA) (http://maps.elie.ucl.ac.be/CCI/viewer/download.php). Soil data with a spatial resolution of 10 km were acquired from the Food and Agriculture Organization (FAO) of the United Nations. Additionally, daily rainfall data in the period 1979–2017 were collected from the Hydro-Meteorological Centre of Southern Vietnam. Additional meteorological data (maximum and minimum temperature, solar radiation, wind speed,

and relative humidity) were automatically generated by a weather generator tool within the SWAT model. The SWAT model utilizes the WXGEN statistical tool as the weather generator to fill the missing meteorological data based on the monthly statistics, which are estimated from existing daily data. The WXGEN model firstly produces the probability of rainfall occurrence for a given day and its corresponding amount. After that, maximum and minimum temperature, solar radiation, and relative humidity are produced based on the presence or absence of rainfall for the day. Lastly, wind speed is independently produced. Further details on the WXGEN weather generator model can be found in Neitsch *et al.* (2011). Daily streamflow data from 1980–1993 were also collected from the Hydro-Meteorological Centre of Southern Vietnam at two stream gauges (Phuoc Long and Phuoc Hoa Stations) of the study region (Figure 1). The observed streamflow data were applied to calibrate and validate the SWAT model.

There are four steps in setting up the SWAT model to simulating streamflow for the studied river basin. The first step is watershed delineation, whereby the BRB was divided into 71 sub-basins through basin configuration and topographical parameterization using the 30 m DEM, and setting the value of 8,000 ha as the threshold area. The second step is to define the HRU. HRU is the smallest unit represented by homogeneous characteristics of land use, slope, and soil type. In this study, 10% was fixed as the threshold value for all three classes. It means that any area with land use, slope or soil type smaller than 10% to the total watershed area is neglected in defining HRU. As the results, 451 HRUs were determined within 71 sub-basins. In the third step, the meteorological data obtained from nine rain gauges (Figure 1) with the essential information of HRU were inputted to the SWAT for running the model. The streamflow was simulated for the past period of 1980–1993 with 1-year warm up for model stabilization. The last step is the calibration and validation processes; hereby, the simulated and observed streamflow at the Phuoc Long and Phuoc Hoa Stations were used for calibration and validation in the two periods of 1980–1990 and 1991–1993, respectively. Calibration and validation of the SWAT model were done using the SWAT-CUP tool (Abbaspour 2015). The tool includes a number of methods for calibration and uncertainty analysis, such as generalized likelihood uncertainty estimation (GLUE), Markov Chain Monte Carlo (MCMC), particle swarm algorithm (PSO), parameter solution (ParaSol), and sequential uncertainty fitting (SUFI-2). Among these methods, the SUFI-2 algorithm is selected to calibrate hydrological simulation in this study because the SUFI-2 can calibrate the model results to be satisfied with a minimum number of iterations (Khoi *et al.* 2017).

The performance of the SWAT model was tested using two model performance indicators given by Moriasi *et al.* (2007), including Nash–Sutcliffe efficiency (NSE) and percent bias (PBIAS), whose definitions are shown as follows:

$$\mathrm{NSE} = 1 - \frac{\sum_{i=1}^{n} (O_i - P_i)^2}{\sum_{i=1}^{n} (O_i - \bar{O})^2} \tag{1}$$

$$\mathrm{PBIAS} = \frac{\sum_{i=1}^{n} (O_i - P_i)}{\sum_{i=1}^{n} O_i} \tag{2}$$

where n is the number of observed data, O_i and P_i are the observed and simulated data at the time i, and $\bar{O}$ is the mean of observed data. As stated by Moriasi *et al.* (2007), the model result is satisfactory once NSE > 0.5 and PBIAS $= \pm 25\%$ for streamflow simulation.

3.2. Downscaling of climate change projections

In order to apply the GCM simulations in a regional scale and generate climate change scenarios for the local assessment of hydrological response, the Long Ashton Research Station Weather Generator (LARS-WG) tool was employed to downscale the simulation information from global scale to local scale. As a statistical downscaling technique, the LARS-WG can simulate meteorological variables based on a series of semi-empirical distributions (Sha *et al.* 2019). More details on the LARS-WG model can be found in Semenov & Barrow (1997). The LARS-WG downscaling technique was selected for this study because of its simplicity in generating climate change scenarios from various GCM simulations. Additionally, numerous previous climate change studies have used this tool to downscale the climatic data from global to local scales (Khoi *et al.* 2019; Sha *et al.* 2019; Ma *et al.* 2021).

In the present study, three future climate change periods were developed corresponding to the 20-year periods of the 2030s (2021–2040), 2050s (2041–2060), and 2070s (2061–2080), using five GCMs (EC-EARTH, GFDL-CM3, HadGEM2-ES, MIROC5, and MPI-ESM-MR) under RCP4.5 and RCP8.5 obtained from the Coupled Model Intercomparison Project 5 (CMIP5). The LARS-WG model conducts two major steps, including calibration and validation, and generating the future climate scenarios. In the calibration and validation step, the LARS-WG performance was evaluated by comparing the values of mean and root mean squared error (RMSE) between simulated and observed data.

3.3. Analysis of hydro-meteorological drought

In this study, two popular indices, namely the SPI and SDI, were used to analyze historical drought conditions and predict future drought in terms of meteorological and hydrological perspectives. The two selected indices are widely used and preferred indices because of their simplicity in the estimation of drought characteristics (Sam *et al.* 2019; Tan *et al.* 2019). The SPI and SDI indices were computed by McKee *et al.* (1993) using monthly precipitation and streamflow as input data, respectively. According to the drought classification of McKee *et al.* (1993) (Table 1), a drought event was identified as the value of SPI or SDI is below −1.

The drought features of the BRB were represented by the two drought indices for 6 months (SPI6 and SDI6). According to Spinoni *et al.* (2014), the hydro-meteorological features are portrayed the best when using 6-month (medium-term) accumulation periods in comparison to 3-month (short-term) or 12-, 24-, and 48-month (long-term) accumulation periods. Therefore, the medium-term accumulation period was used in this study. In the drought features, three aspects were considered for the present study, including drought frequency (the number of months with the SPI or SDI values below −1 over a specified period), drought duration (the number of months with the values of SPI or SDI consecutively below −1), and drought severity (the average values of SPI or SDI throughout the drought duration).

The relationship between the drought and global climate oscillation (ENSO and PDO) was quantitatively estimated using the Pearson's correlation coefficient (CC). The positive value of CC shows a direct correlation and the negative value of CC shows an inverse correlation. In this study, the bi-monthly multivariate ENSO index (MEI.v2) and PDO were obtained from the Physical Sciences Laboratory (PSL) of National Oceanic and Atmospheric Administration (NOAA) (https://psl.noaa.gov/data/climateindices/list/).

4. RESULTS AND DISCUSSION

4.1. Performance evaluation of the SWAT model

Calibration and validation of the SWAT model were conducted to ensure that the simulation of hydrological processes is reasonably good for estimating the SDI index. The periods of 1980–1989 and 1990–1993 were used for the SWAT calibration and validation, respectively. Figure 2 shows the calibration and validation results of the streamflow simulation at the Phuoc Long and Phuoc Hoa stations. General speaking, the model performed well in simulating the streamflow trend in the both calibration and validation periods. However, the SWAT model has not always captured well the peak of the flows, which might be caused by the simplification of the hydrological model and heterogeneous spatial distribution of precipitation. Additionally, Table 2 presents the statistical results of the SWAT performance in the streamflow simulations. The simulated

Table 1 | Categorization of drought using the SPI and the SDI

Range	Categorization
SPI, SDI $\geq +2.0$	Extremely wet condition
$1.5 \leq$ SPI, SDI < 2.0	Very wet condition
$1.0 \leq$ SPI, SDI < 1.5	Moderately wet condition
$-1.0 \leq$ SPI, SDI < 1.0	Normal condition
$-1.5 \leq$ SPI, SDI < -1.0	Moderate drought
$-2.0 \leq$ SPI, SDI < -1.5	Severe drought
SPI, SDI ≤ -2.0	Extreme drought

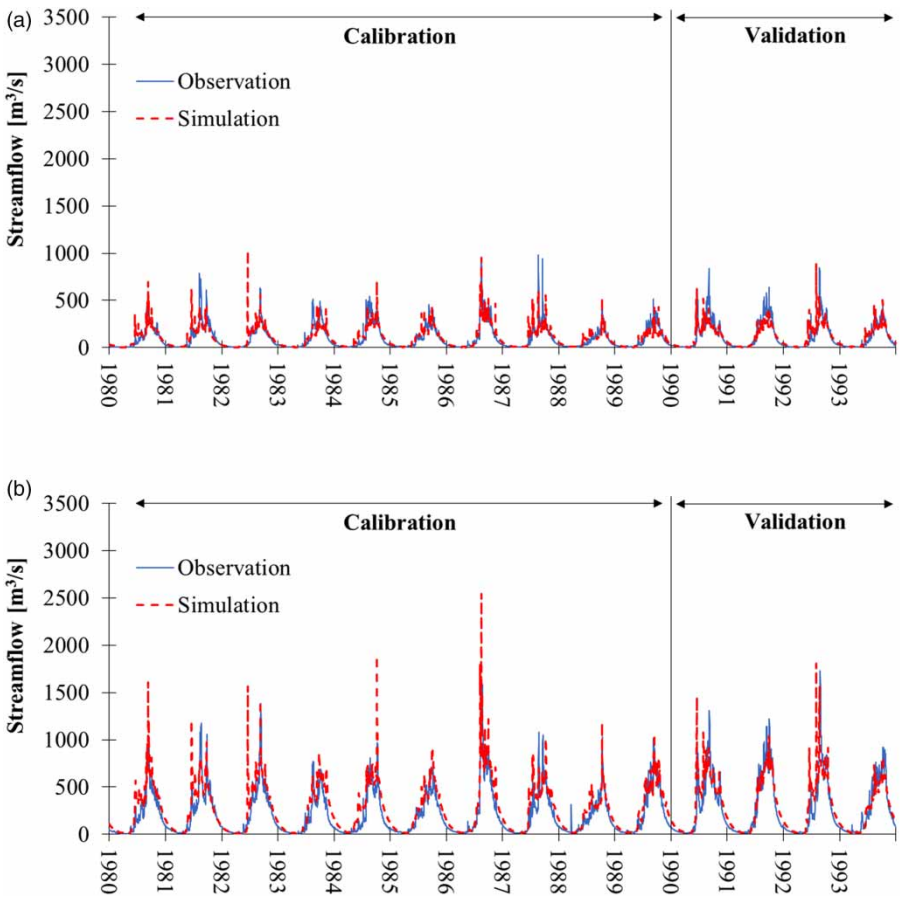

Figure 2 | Monthly streamflow hydrographs of calibration and validation periods comparing observed and simulated values at the two stream gauges in the BRB. (a) Phuoc Long Station. (b) Phuoc Hoa Station.

Table 2 | Model performance statistics for the simulation of daily and monthly streamflow

		Daily simulation		Monthly simulation	
	Time period	NSE	PBIAS	NSE	PBIAS
Phuoc Long	Calibration: 1980–1990	0.74	6.4%	0.86	6.1%
	Validation: 1991–1993	0.78	3.3%	0.95	2.9%
Phuoc Hoa	Calibration: 1980–1990	0.73	−25.4%	0.86	−25.1%
	Validation: 1991–1993	0.83	−5.3%	0.98	−4.9%

values are fitted well to the observed values of streamflow proven by the NSE and PBIAS values varying in the range of 0.73 to 0.83 and −25 to 6% for the daily simulation; and 0.86 to 0.98 and −25 to 6% for the monthly simulation for both calibration and validation periods, respectively. Overall, based on the statistical indices as shown in Table 2, the values of NSE > 0.5 and PBIAS = ±25% (Moriasi *et al.* 2007) indicate the reasonable performance of the SWAT model for the study area. Thus, the calibrated SWAT model can simulate the streamflow for the Be River to assess the effect of climate change on streamflow and hydrological drought.

4.2. Identification of historical drought characteristics

Using the two drought indices, namely SPI and SDI, the historical drought conditions during 1980–2017 were evaluated. Figure 3 shows the variation of drought severity estimated from the SPI6 and SDI6 time series (6-month accumulation

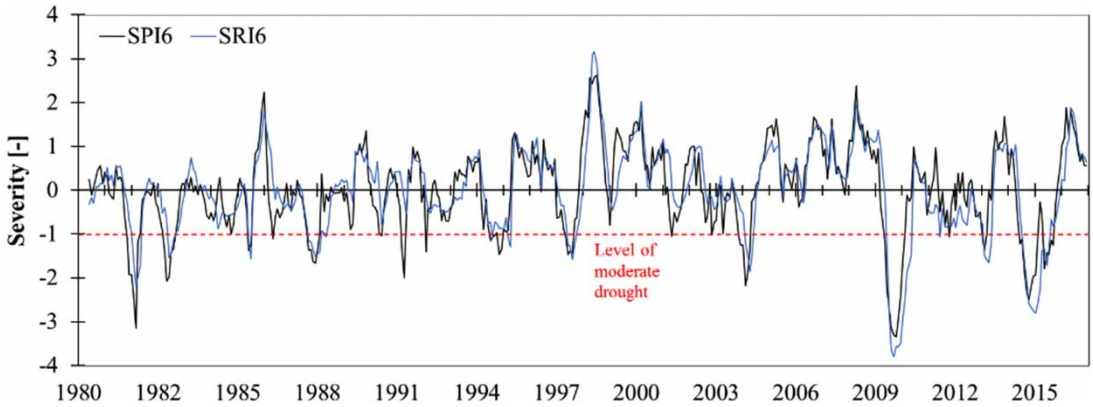

Figure 3 | Temporal variation of SPI6 and SDI6 over the BRB in the period 1980–2017.

period). The figure illustrated that the SPI6 and SDI6 indices have the similar trends of severity and drought timing. Further, the figure exhibited that the drought frequency in the period 1980–2005 is larger than that in the period 2005–2017, but the drought severity in the period 1980–2005 is smaller than that in the period 2005–2017. Based on the recorded severe droughts (World Bank 2019), the SPI and SDI indices showed a good agreement between estimated and observed data, with especially severe drought events during the years 1997/1998, 2004/2005, 2010/2011, and 2015/2016.

Table 3 presents the Pearson's CC values of SPI6 with SDI6 as well as drought indices with global climate oscillation at different lag times. The table presents that SPI6 had a highest CC value of 0.90 with a 1-month lagged SDI6. This implies that the hydrological drought has a 1-month lag time from the meteorological drought. It is reasonable that streamflow lag after climatic variation and the length of time lag is controlled by climatic and basin characteristics (Kamali *et al.* 2017). Sam *et al.* (2019) also described the same type of result in the Central Highlands of Vietnam. Additionally, the global climate oscillation (MEIv2 and PDO) had negative correlations with the SPI6 and SDI6 indices (Table 3). This indicates that the decreases in the SPI and SDI values are related to increases in the El Niño and PDO warm phases, and consequently rises in the possibility of meteorological and hydrological droughts. Similarly, Stojanovic *et al.* (2020) also indicated negative correlations of meteorological drought with the ENSO and PDO in South Vietnam. Table 3 also shows that the meteorological drought has a 7-month lag time from the ENSO and 8-month lag time from the PDO, and the hydrological drought has an 8-month lag time from the ENSO and a 9-month lag time from the PDO. Furthermore, the correlation between the drought indices and ENSO was more powerful than that between the drought indices and PDO. Nalley *et al.* (2019) indicated that the considerable effect of ENSO was reflected in the variability of regional hydrological processes, such as precipitation and streamflow.

4.3. Projected changes in precipitation and streamflow

The LARS-WG performance in the simulation of monthly precipitation for the period 1986–2005 is exhibited in Table 4. It presents that the average monthly precipitation between simulation and observation are quite consistent over all rain gauges, and the differences between monthly simulated and observed precipitation ranged from 1 to 39 mm/month for the

Table 3 | The Pearson's CC of drought indices with global climate oscillation at different lag times for the period 1980–2017

	Lag time (months)										
	0	1	2	3	4	5	6	7	8	9	10
SPI6 vs. SDI6	0.85	0.90	0.86	0.78	0.67	0.54	0.39	0.24	0.13	0.04	−0.04
MEIv2 vs. SPI6	−0.13	−0.17	−0.21	−0.26	−0.29	−0.32	−0.34	−0.36	−0.35	−0.34	−0.31
MEIv2 vs. SDI6	0.02	−0.02	−0.06	−0.11	−0.16	−0.21	−0.25	−0.28	−0.31	−0.29	−0.25
PDO vs. SPI6	−0.12	−0.13	−0.15	−0.18	−0.21	−0.23	−0.25	−0.25	−0.26	−0.24	−0.21
PDO vs. SDI6	−0.07	−0.09	−0.09	−0.10	−0.12	−0.14	−0.16	−0.18	−0.20	−0.21	−0.19

Table 4 | The LARS-WG performance statistics for simulation of monthly precipitation in the period 1986–2005

Station		Phuoc Long	Dong Phu	Dak Nong	Binh Long	Bu Dop	Bu Nho	Chon Thanh	Phuoc Hoa	So Sao
Calibration (1986–1995)	Obs. (mm)	261	249	229	199	309	240	195	186	166
	Sim. (mm)	266	253	237	238	316	243	196	206	179
	RMSE (mm)	140	140	134	151	166	167	130	106	98
	R^2	0.73	0.68	0.67	0.61	0.61	0.56	0.57	0.76	0.70
Validation (1996–2005)	Obs. (mm)	245	236	236	226	249	234	182	194	164
	Sim. (mm)	266	253	237	238	316	243	196	206	179
	RMSE (mm)	144	136	154	174	192	143	143	109	119
	R^2	0.52	0.50	0.46	0.50	0.51	0.48	0.48	0.61	0.53

calibration, and 1 to 67 mm/month for the validation. Concerning the correlation between observed and simulated monthly precipitation, the R^2 values are reasonable and varied from 0.56 to 0.76 and 0.46 to 0.61 in the calibration and validation periods. Furthermore, the RMSE values ranged from 98 to 167 mm and 109 to 174 mm for the calibration and validation periods. The LARS-WG performance statistics for the BRB were sufficiently good, and the statistics are compatible with previous studies of Agarwal *et al.* (2014) and Hassan *et al.* (2014). Therefore, the well-calibrated and -validated model has great capacity for simulating the monthly precipitation data under the future climate scenarios for all nine rain gauges in the present study.

Five GCMs (EC-EARTH, GFDL-CM3, HadGEM2-ES, MIROC5, and MPI-ESM-MR) driven by the RCP4.5 and RCP8.5 emission scenarios were selected to project the future precipitation. Considering the ensemble mean of five GCMs, the future changes in precipitation with respect to the baseline time period over the BRB are presented in Figure 4. The yearly precipitation will experience a reduction of 4.0% during the 2030s and rises of 1.6 and 6.4% during the 2050s and 2070s for the RCP4.5. Regarding the RCP8.5, the yearly precipitation will undergo reductions of 4.5 and 0.6% during the 2030s and 2050s; and a rise of 5.1% during the 2070s. In terms of seasonal variation, the change patterns of wet-seasonal precipitation are almost identical to those of yearly precipitation for the both RCP4.5 and RCP8.5. The changes in wet-seasonal precipitation range from −5.5 to 2.9% for the RCP4.5 and −5.0 to 1.2% for the RCP8.5. The dry-seasonal precipitation is projected to rise inside the ranges of 5.9–27.9% for the RCP4.5 and −1.1–29.2% for the RCP8.5.

The projected streamflow in the BRB will generally undergo a rise in the near future period and reductions in the following future periods compared with the baseline time period, which corresponds to the projected changes in precipitation. Specifically, the yearly streamflow will undergo changes of −7.1, 1.2, and 8.5% for the RCP4.5 and −7.0, −2.9, and 4.2% for the RCP8.5 during the 2030s, 2050s, and 2070s, respectively. The future changes in monthly streamflow with respect to the baseline time period over the BRB are illustrated in Figure 5. Considering the seasonal change of projected streamflow, the streamflow will experience changes of −8.0 to 7.4% for the RCP4.5 and −7.7 to 3.5% for the RCP8.5 in the wet season and rises of 1.2–14.9% for the RCP4.5 and 3.2–7.9% in the RCP8.5 in the dry season.

4.4. Projected changes in the hydro-meteorological droughts

The projected changes in duration, severity, and frequency of the meteorological and hydrological droughts over the study area are shown in Table 5. Corresponding to the projected changes in yearly precipitation, the frequency of meteorological

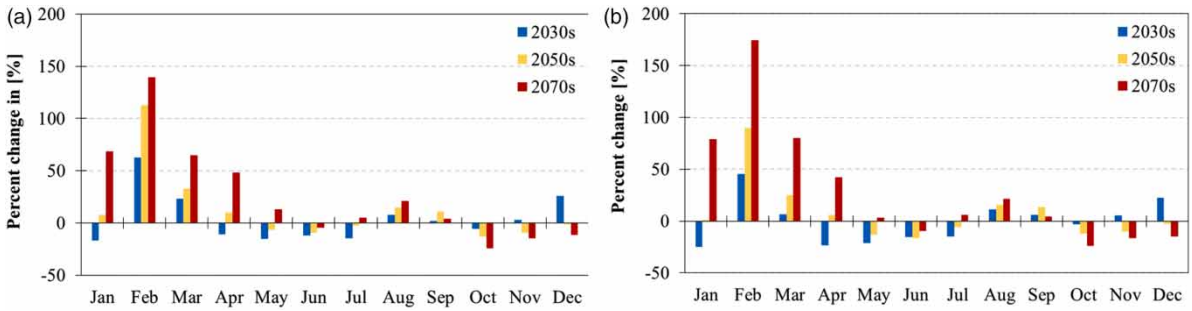

Figure 4 | Projected changes in monthly precipitation over the BRB. (a) RCP4.5 scenario. (b) RCP8.5 scenario.

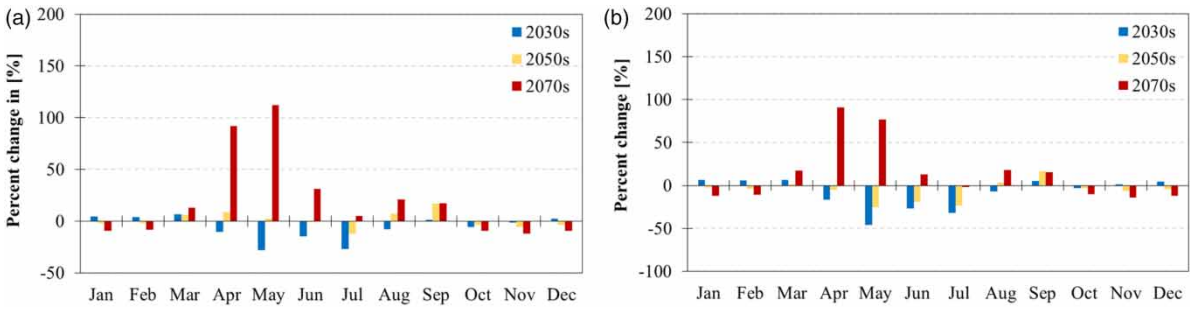

Figure 5 | Projected changes in monthly streamflow over the BRB. (a) RCP4.5 scenario. (b) RCP8.5 scenario.

drought is expected to have a rise of 14.2% during the 2030s and reductions of −5.2 and −13.7% during the 2050 and 2070s for the RCP4.5. Regarding the RCP8.5, the drought frequency has rising trends of 20.5 and 8.8% during the 2030s and 2050s and a downward trend of −17.6% during the 2070s. Under the climate change impacts, the drought severity will experience small reductions within the range of −5.8 to −1.4%, and the drought duration will undergo changes within the bounds of −5.2 to 13.2% for both RCP4.5 and RCP8.5.

In terms of hydrological drought, the drought frequency is projected to have a rise of 34.5% during the 2030s and reductions of −13.8 and −44.8% during the 2050s and 2070s for the RCP4.5. Concerning the RCP8.5, rising trends of 20.7 and 3.5% during the 2030s and 2050s and a downward trend of −10.3% during the 2070s are predicted for the drought frequency. Generally, the frequency of hydro-meteorological drought will undergo rising trends in the near future period and downward trends in the following future periods. Similarly, Sam *et al.* (2019) also reported rising trends in the drought frequency in the near future period of 2016–2040 in the Central Highlands of Vietnam. Regarding the drought duration, it is predicted to have significant changes varying from −21.4 to 18.8% for the both RCP4.5 and RCP8.5. Similar to projected reduction in the severity of the meteorological drought, the severity of hydrological drought will also undergo reductions of −11.4 to −8.4% for the RCP4.5 and −15.8 to −9.0% for the RCP8.5. The reductions in the meteorological and hydrological severity may be associated with rises in the dry-seasonal precipitation and streamflow. Similar to this finding, the drought severity is also subjected to downward trends in the future in the Dakbla River Basin, which is a neighbor river basin of the study region (Vu *et al.* 2015).

In the face of more frequent drought in the near future, local authorities in the BRB should improve the water resource management of the study area to reduce the drought-inflicted risk. Specifically, maintenance and upgrading of the reservoir, and improving the efficiency of irrigation systems should be implemented in the near future. In addition, crop restructuring and use of drought-resistant crops can be applied to respond to droughts. Furthermore, appropriate drought management strategies and climate smart agriculture practices should be promoted to reduce vulnerability of agricultural livelihoods and food security. Applications of climate smart agricultural practices (i.e., farm-level adoption of agroforestry and use of

Table 5 | Projected changes in drought characteristics over the Be River Catchment

	RCP4.5			RCP8.5		
	2030s	2050s	2070s	2030s	2050s	2070s
Meteorological drought (SPI6)						
Duration	10.9%	−5.2%	−13.7%	3.9%	−2.5%	13.2%
Severity	−1.4%	−2.2%	−3.6%	−2.9%	−5.8%	−5.1%
Frequency	14.2%	−5.9%	−23.5%	20.5%	8.8%	−17.6%
Hydrological drought (SDI6)						
Duration	8.3%	−10.9%	−21.4%	1.92%	−11.30%	18.8%
Severity	−8.1%	−11.4%	−10.2%	−9.0%	−11.4%	−15.8%
Frequency	34.5%	−13.8%	−44.8%	20.7%	3.5%	−10.3%

drought-resistant crops) can provide long-term benefits, such as diversified farmer incomes, reduced soil erosion, and increased efficiency of water use.

5. CONCLUSIONS

The present study aims to investigate the responses of meteorological and hydrological droughts to changing climate scenarios in the BRB utilizing the SWAT hydrological model, LARS-WG downscaling tool, and drought indices. Three significant conclusions can be drawn from this study: (1) the analysis of the hydro-meteorological droughts in the historical period indicated that a 1-month lag time between hydrological drought and meteorological drought was determined, and the hydro-meteorological droughts have negative correlations with the ENSO and PDO; (2) under the climate change impact, the projected precipitation and streamflow in the BRB will generally increase in the near future period (2030s) and reduce in the following future periods (2050 and 2070s) in comparison to the baseline period; and (3) the hydro-meteorological drought of the study area will be moderated by downward trends in severity in the future. But the drought frequency will have experience of a rising trend in the near future period and downward trends in the following future periods. The findings drawn from this research could give more knowledge for enhancing the understanding of the hydro-meteorological drought conditions under various climate change scenarios. Consequently, the policy- and decisionmakers can propose the water resource management and water supply plan which is more appropriate to this region.

AUTHOR CONTRIBUTIONS

D.N.K. and V.T.N. conceptualized the whole article. D.N.K. and B.V.H. performed data acquisition. D.N.K. and T.T.S. carried out formal analysis. D.N.K. involved in funding acquisition. D.N.K. and B.V.H. investigated the study. D.N.K. and V.T.N. developed the methodology. P.T.L. and T.T.S. studied software. D.N.K. and V.T.N. supervised the study. All authors have read and agreed to the published version of the manuscript.

ACKNOWLEDGEMENTS

This research is funded by Vietnam National University Ho Chi Minh City (VNU-HCM) under grant no. B2019-18-07. The authors also would like to thank the anonymous reviewers for their valuable and constructive comments to improve our manuscript.

CONFLICTS OF INTEREST

The authors declare no conflict of interest.

DATA AVAILABILITY STATEMENT

All relevant data are included in the paper or its Supplementary Information.

REFERENCES

Abbaspour, K. C. 2015 *SWAT-CUP: SWAT Calibration and Uncertainty Programs-A User Manual*. Eawag – Swiss Federal Institute of Aquatic Science and Technology, Dübendorf, Switzerland.

Agarwal, A., Babel, M. S. & Maskey, S. 2014 Analysis of future precipitation in the Koshi river basin, Nepal. *Journal of Hydrology* **513**, 422–434. doi:10.1016/j.jhydrol.2014.03.047.

Blanco-Gómez, P., Jimeno-Sáez, P., Senent-Aparicio, J. & Pérez-Sánchez, J. 2019 Impact of climate change on water balance components and droughts in the Guajoyo River Basin (El Salvador). *Water* **11**, 2360. doi:10.3390/w11112360.

Eckstein, D., Kunzel, V. & Schafer, L. 2021 *Global Climate Risk Index 2021: Who Suffers Most From Extreme Weather Events? Weather-Related Loss Events in 2019 and 2000 to 2019*. Germanwatch e.V., Bonn, Germany.

Hassan, Z., Shamsudin, S. & Harun, S. 2014 Application of SDSM and LARS-WG for simulating and downscaling of rainfall and temperature. *Theoretical and Applied Climatology* **116**, 243–257. doi:10.1007/s00704-013-0951-8.

IPCC 2013 *Climate Change 2013, the Physical Science Basis*. Cambridge University Press, Cambridge, UK.

IPCC 2018 *Global Warming of 1.5°C. An IPCC Special Report on the Impacts of Global Warming of 1.5°C Above pre-Industrial Levels and Related Global Greenhouse gas Emission Pathways, in the Context of Strengthening the Global Response to the Threat of Climate Change* (Masson-Delmotte, V., Zhai, P., Pörtner, H.-O., Roberts, D., Skea, J., Shukla, P. R., Pirani, A., Moufouma-Okia, W., Péan, C., Pidcock, R., Connors, S., Matthews, J. B. R., Chen, Y., Zhou, X., Gomis, M. I., Lonnoy, E., Maycock, T., Tignor, M. & Waterfield, T., eds). In Press. https://www.ipcc.ch/site/assets/uploads/sites/2/2019/06/SR15_Full_Report_High_Res.pdf.

Jung, I. W. & Chang, H. 2012 Climate change impacts on spatial patterns in drought risk in the Willamette River Basin, Oregon, USA. *Theoretical and Applied Climatology* **108**, 355–371. doi:10.1007/s00704-011-0531-8.

Kamali, B., Houshmand Kouchi, D., Yang, H. & Abbaspour, K. 2017 Multilevel drought hazard assessment under climate change scenarios in semi-srid regions – A case study of the Karkheh River Basin in Iran. *Water* **9**, 241. doi:10.3390/w9040241.

Khoi, D. N., Thom, V. T., Quang, C. N. X. & Phi, H. L. 2017 Parameter uncertainty analysis for simulating streamflow in the upper Dong Nai river basin. *La Houille Blanche* 14–23. doi:10.1051/lhb/2017003.

Khoi, D. N., Sam, T. T., Nhi, P. T. T., Quan, N. T., Hung, B. V., Phung, N. K. & Nguyen, V. T. 2019 Uncertainty assessment for climate change impact on streamflow and water quality in the Dong Nai River Basin, Vietnam. In: *World Environmental and Water Resources Congress 2019* (Scott, G. F. & Hamilton, W., eds). American Society of Civil Engineers, Reston, VA, pp. 366–373. doi:10.1061/9780784482346.037.

Ma, D., Budong, Q., Gu, H., Sun, Z. & Xu, Y. P. 2021 Assessing climate change impacts on streamflow and sediment load in the upstream of the Mekong River Basin. *International Journal of Climatology*. joc.7025. doi:10.1002/joc.7025.

McKee, T. B., Doesken, N. J. & Kliest, J. 1993 The relationship of drought frequency and duration to time scales. In: *Proceedings of the 8th Conference on Applied Climatology*. Boston, pp. 179–184.

Moriasi, D. N., Arnold, J. G., Van Liew, M. W., Bingner, R. L., Harmel, R. D. & Veith, T. L. 2007 Model evaluation guidelines for systematic quantification of accuracy in watershed simulations. *Transactions of the ASABE* **50**, 885–900.

Nalley, D., Adamowski, J., Biswas, A., Gharabaghi, B. & Hu, W. 2019 A multiscale and multivariate analysis of precipitation and streamflow variability in relation to ENSO, NAO and PDO. *Journal of Hydrology* **574**, 288–307. doi:10.1016/j.jhydrol.2019.04.024.

Neitsch, A. L., Arnold, J. G., Kiniry, J. R. & Williams, J. R. 2011 *Soil and Water Assessment Tool: Theoretical Documentation Version 2009*. Texas A&M University, Texas.

Prudhomme, C., Giuntoli, I., Robinson, E. L., Clark, D. B., Arnell, N. W., Dankers, R., Fekete, B. M., Franssen, W., Gerten, D., Gosling, S. N., Hagemann, S., Hannah, D. M., Kim, H., Masaki, Y., Satoh, Y., Stacke, T., Wada, Y. & Wisser, D. 2014 Hydrological droughts in the 21st century, hotspots and uncertainties from a global multimodel ensemble experiment. *Proceedings of the National Academy of Sciences* **111**, 3262–3267. doi:10.1073/pnas.1222473110..

Salimi, H., Asadi, E. & Darbandi, S. 2021 Meteorological and hydrological drought monitoring using several drought indices. *Applied Water Science* **11**, 11. doi:10.1007/s13201-020-01345-6.

Sam, T. T., Khoi, D. N., Thao, N. T. T., Nhi, P. T. T., Quan, N. T., Hoan, N. X. & Nguyen, V. T. 2019 Impact of climate change on meteorological, hydrological and agricultural droughts in the Lower Mekong River Basin: a case study of the Srepok Basin, Vietnam. *Water and Environment Journal* **33**, 547–559. doi:10.1111/wej.12424.

Semenov, M. A. & Barrow, E. M. 1997 Use of a stochastic weather generator in the development of climate change scenarios. *Climatic Change* **35**, 397–414. doi:10.1023/A:1005342632279.

Sha, J., Li, X. & Wang, Z. L. 2019 Estimation of future climate change in cold weather areas with the LARS-WG model under CMIP5 scenarios. *Theoretical and Applied Climatology* **137**, 3027–3039. doi:10.1007/s00704-019-02781-4.

Spinoni, J., Naumann, G., Carrao, H., Barbosa, P. & Vogt, J. 2014 World drought frequency, duration, and severity for 1951–2010. *International Journal of Climatology* **34**, 2792–2804. doi:10.1002/joc.3875.

Stojanovic, M., Liberato, M. L. R., Sorí, R., Vázquez, M., Phan-Van, T., Duongvan, H., Hoang Cong, T., Nguyen, P. N. B., Nieto, R. & Gimeno, L. 2020 Trends and extremes of drought episodes in Vietnam Sub-Regions during 1980–2017 at different timescales. *Water* **12**, 813. doi:10.3390/w12030813.

Tan, M. L., Juneng, L., Tangang, F. T., Chan, N. W. & Ngai, S. T. 2019 Future hydro-meteorological drought of the Johor River Basin, Malaysia, based on CORDEX-SEA projections. *Hydrological Sciences Journal* **64**, 921–933. doi:10.1080/02626667.2019.1612901.

Tan, M. L., Gassman, P. W., Yang, X. & Haywood, J. 2020 A review of SWAT applications, performance and future needs for simulation of hydro-climatic extremes. *Advances in Water Resources* **143**, 103662. doi:10.1016/j.advwatres.2020.103662.

UNDP 2016 *Viet Nam Drought and Saltwater Intrusion: Transforming From Emergency to Recovery*. Analysis Report and Policy Implications, Hanoi, Vietnam.

Vu, M. T., Raghavan, V. S. & Liong, S.-Y. 2015 Ensemble climate projection for hydro-meteorological drought over a river basin in Central Highland, Vietnam. *KSCE Journal of Civil Engineering* **19**, 427–433. doi:10.1007/s12205-015-0506-x.

Vu-Thanh, H., Ngo-Duc, T. & Phan-Van, T. 2014 Evolution of meteorological drought characteristics in Vietnam during the 1961–2007 period. *Theoretical and Applied Climatology* **118**, 367–375. doi:10.1007/s00704-013-1073-z.

World Bank 2019 *Striking A Balance: Managing El Niño and La Niña in Vietnam's Agriculture*. The World Bank, Washington, DC, USA.

World Bank, and GFDRR 2017 *Toward Integrated Disaster Risk Management in Vietnam. Recommendations Based on the Drought and Saltwater Intrusion Crisis and the Case for Investing in Longer-Term Resilience*. The Publishing and Knowledge Division, The World Bank, Washington, DC, USA.

World Economic Forum 2021 *The Global Risks Report 2021*. World Economic Forum, Geneva, Switzerland.

Wu, J., Chen, X., Yao, H., Gao, L., Chen, Y. & Liu, M. 2017 Non-linear relationship of hydrological drought responding to meteorological drought and impact of a large reservoir. *Journal of Hydrology* **551**, 495–507. doi:10.1016/j.jhydrol.2017.06.029.

Zhao, P., Lü, H., Yang, H., Wang, W. & Fu, G. 2019 Impacts of climate change on hydrological droughts at basin scale: a case study of the Weihe River Basin, China. *Quaternary International* **513**, 37–46. doi:10.1016/j.quaint.2019.02.022.

First received 4 April 2021; accepted in revised form 6 June 2021. Available online 21 June 2021